A dynamic building and aquifer co-simulation method for thermal imbalance investigation

Bozkaya, Basar; Li, Rongling; Zeiler, Wim

Published in:
Applied Thermal Engineering

Link to article, DOI:
10.1016/j.applthermaleng.2018.08.095

Publication date:
2018

Document Version
Publisher's PDF, also known as Version of record

Applied Thermal Engineering 144 (2018) 681–694

Contents lists available at ScienceDirect

Applied Thermal Engineering

journal homepage: www.elsevier.com/locate/apthermeng

A dynamic building and aquifer co-simulation method for thermal imbalance investigation

Basar Bozkaya[a,*], Rongling Li[b], Wim Zeiler[a]

[a] Department of Built Environment, Eindhoven University of Technology, De Zaale, PO Box 513, 5600 MB Eindhoven, The Netherlands
[b] Department of Civil Engineering, Technical University of Denmark, 2800 Kgs. Lyngby, Denmark

HIGHLIGHTS

- A co-simulation tool including COMSOL-MATLAB-TRNSYS was developed and applied.
- Thermal imbalance problem of ATES was investigated for cooling dominated loads.
- The cold well temperature was decreased by 2.5 °C by maintaining a thermal balance.
- Thermally balanced building performed up to 13.7% higher performance.

ARTICLE INFO

Keywords:
Aquifer thermal
Aquifer thermal energy storage
Co-simulation
Thermal imbalance
Underground thermal energy storage

ABSTRACT

Due to their favorable supply temperature, aquifer thermal energy storage (ATES) systems perform as an efficient heating/cooling energy storage facility for buildings. ATES systems consist of a warm and cold well. They are designed to operate with a temperature difference of at least 8 °C between wells, whereas the existing installations operate in practice with an average temperature difference of 4 °C. The ATES supply temperature is influenced by heat losses to the surroundings and the yearly balance of total heat exchange of heating and cooling between a building and the groundwater. Previous studies mainly focused on the investigation of heat losses to the environment. This paper explored the influence of thermal imbalance of a building load on the temperature of the aquifer and the heating/cooling system performance for the building. Due to the lack of tools capable of simulating the system that connects ATES with the buildings, we develop a co-simulation method that combines COMSOL, MATLAB and TRNSYS. In this method, COMSOL was used to model ATES, TRNSYS to simulate buildings and heating, ventilation and air conditioning (HVAC) systems and MATLAB as a mediator to exchange information between the simulation tools. The developed method was applied to a case study with three different insulation parameters to present different thermal load profiles. The results indicated that a thermally balanced building load achieved a 2.5 °C higher temperature difference between the sources for cooling than a case with a thermal imbalance ratio of 79%, which resulted in a 13.7% and 6% higher system coefficient of performance (COP) higher than the case with 79% thermal imbalance ratio and 51% thermal imbalance ratio, respectively.

1. Introduction

Energy consumption in buildings has been inevitably increasing for the last several decades. Heating and cooling systems are responsible for the majority of the energy use within a building. As a result, numerous underground thermal storage systems have been introduced as energy-efficient sources for heating and cooling applications in combination with a heat pump, due to the suitable and stable supply temperature.

Commonly, there are two underground thermal storage systems that have inter-seasonal operation. One is borehole thermal energy storage (BTES), and the other is aquifer thermal energy storage (ATES). In the BTES system, heat is exchanged with the ground through closed-loop pipes by means of conduction. ATES utilizes readily available groundwater to transport heat to a building using an open-loop pipe system. The exchanged heat is stored in the same storage field throughout the season in a BTES system, while it is stored separately using doublet wells in an ATES system: in a cold well in the winter and a warm well in

* Corresponding author.
E-mail address: b.bozkaya@tue.nl (B. Bozkaya).

https://doi.org/10.1016/j.applthermaleng.2018.08.095
Received 12 February 2018; Received in revised form 20 July 2018; Accepted 26 August 2018
Available online 28 August 2018

Nomenclature

K	hydraulic conductivity (m/s)
h	hydraulic head (m)
	flow flux (m^2/s)
ρ	density (kg/m^3)
S_s	storage term
Q_s	source term (m^3/s)
K	hydraulic conductivity (m/s)
$(pc)_f$	specific heat capacity of fluid $(kJ/kg°C)$
$(pc)_{aq}$	specific heat capacity of aquifer $(kJ/kg°C)$
λ_{aq}	thermal conductivity of aquifer (mC/kJ)
Q_{inj}	injected heat to the ground (kJ)_
Q_{ext}	extracted heat from the ground(kJ)
T_{ww}	extraction temperature from the warm well $(°C)$
V_{max}	maximum flow rate of water (kg/hr)
Q_b	heat transfer to the building (kJ)
COP_{HPC}	COP cooling supply in heat pump mode
COP_{direct}	COP of direct cooling supply
$COP_{cooling}$	cooling COP
$COP_{heating}$	heating COP
COP_{sys}	system COP
Q_{hpc}	cooling supply to the building (HP mode) (kJ)
Q_{dc}	cooling supply to the building (DC mode) (kJ)
Q_{cool}	total cooling supply to the building (kJ)
$W_{pump,cw}$	electricity consumption of cold well pump (kJ)
$W_{pump,ww}$	electricity consumption of warm well pump (kJ)
T_{cw}	extraction temperature from the cold well $(°C)$
$W_{pump,cw}$	electricity consumption of cold well (kJ)
W_{max}	maximum pump electricity consumption (kJ)

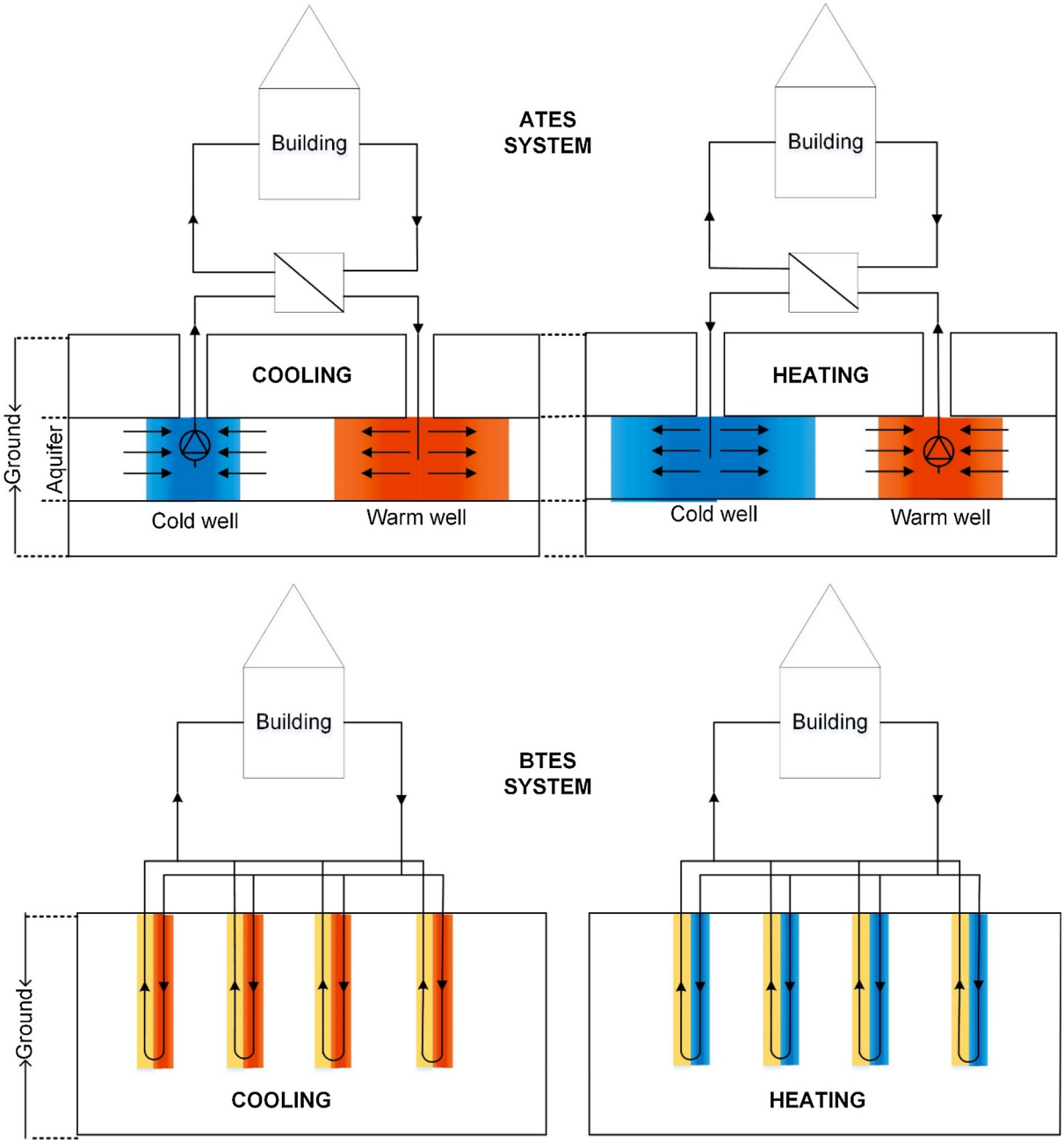

Fig. 1. The principles of ATES and BTES systems (modified from [1]).

the summer. Therefore, there is no direct thermal interaction between sources, as in BTES systems (Fig. 1). In ATES systems, the warm and cold well are designed to maintain a temperature difference of 8 °C between each other to operate energy efficiently. The system is usually designed to operate with an injection temperature of between 6 and 8 °C in the cold well and 16–18 °C in the warm well for a ground temperature of 12 °C in the Netherlands. However, current installations operate with an average temperature difference of 4 °C [1,2], thus the expected operating temperature level is practically not achieved. This influences the overall system energy performance negatively. Well temperature varies throughout the year due to the heat loss to the environment and the amount of injected heat to warm and cold wells. Since, in most cases, buildings have different thermal load patterns (cooling/heating domination), there is an unbalanced heat injection to the cold and the warm well, which influences the temperature in those wells

Following the implementation of recent building energy regulations, buildings are now constructed with much improved insulation techniques and air tightness, which has resulted in increased cooling demand. Depending on the building's structure and internal heat gain, cooling demand can exceed heating demand in buildings in central and northern Europe, especially in non-residential buildings. Specifically, the ATES concept with heat pumps is able to provide highly efficient cooling performance [3-6] and is thus frequently applied in the Netherlands, where there is a cooling domination in the office building load. In the future, ATES systems are therefore expected to be increasingly applied in buildings with a higher need for cooling than for heating [1]; thus, cooling domination in a building load is inevitable for ATES systems.

Thermal imbalance is a problem for both ATES and BTES systems for ground-sourced applications that have inter-seasonal operation. This problem has been intensively studied for BTES systems in several studies [7–13] and studies [7–13] conclude that system performance decreases over time and even results in system failures in heating/cooling supply as a result of the thermal imbalance due to the change in overall supply temperature from the ground.

However, the thermal imbalance problem has not been studied in an ATES context. Studies of ATES systems [14–17] have mainly focused on the thermal modeling of ATES to determine the effect of ground conditions on heat recovery and temperature distribution in the well. Thermal models are significant for correctly characterizing the thermal response of the ground; however, it is not possible to accurately determine temperature levels disconnected from the building load due to the differences in the amount heat extraction. The studies concerning ATES connected to a building are limited to mostly to the experimental data analysis [5,6,18,19] due to the lack of commercial or non-commercial simulation tools.

Taking into account the thermal imbalance problem and the lack of available simulation tools for ATES, in this study, we explored the influence of thermal imbalance on the supply temperature from ATES and the performance of ATES connected to the building load. Therefore, we first develop a co-simulation platform that is able to simulate ATES connected to a building load. Later, the developed model is applied to a building for three different U-values that represent three different thermal imbalance ratios. Correspondingly, the influence of each thermal imbalance ratio on temperature levels and performance of the system is determined.

The subsequent sections of this paper are as follows. Section 2 is a literature survey on previous studies of ATES and BTES; Section 3 provides the methodology and a description of the case study and the co-simulation platform; Section 4 provides the results; Section 5 discusses the results; and Section 6 provides the conclusions.

2. Literature review

Studies concerning the performance analysis of an ATES system have been found to be limited. Existing studies concerning ATES connected to a building load have been conducted to determine the overall performance of the ATES system using experimental data [5,6,18,19] and some simulations [6,20–22]. D. Vanhoudt et al. [5] extensively compare an existing HVAC system with an ATES system in terms of operational cost and COP using the experimental data from the building. They determine that by applying ATES, 71% of the primary energy use can be reduced. Paksoy et al. [18] show that ATES can maintain a 60% higher COP than a conventional cooling system in a supermarket in Turkey. Turgut et al. [19] determine energy cost savings of 70% when ATES is used for heating a greenhouse in comparison to fuel oil. Kranz et al. [6] conduct an experimental analysis and a parametric study to determine the optimal operational parameters for an ATES system. The COP of the system is considerably influenced by the temperature level of the cooling network and the threshold temperature for regeneration of ATES using an air-water heat exchanger [21]. Ghaebi evaluates the performance of ATES's various operation modes: ATES for only cooling, ATES for heating connected to solar thermal and ATES for both heating and cooling. The analysis shows that the COP for

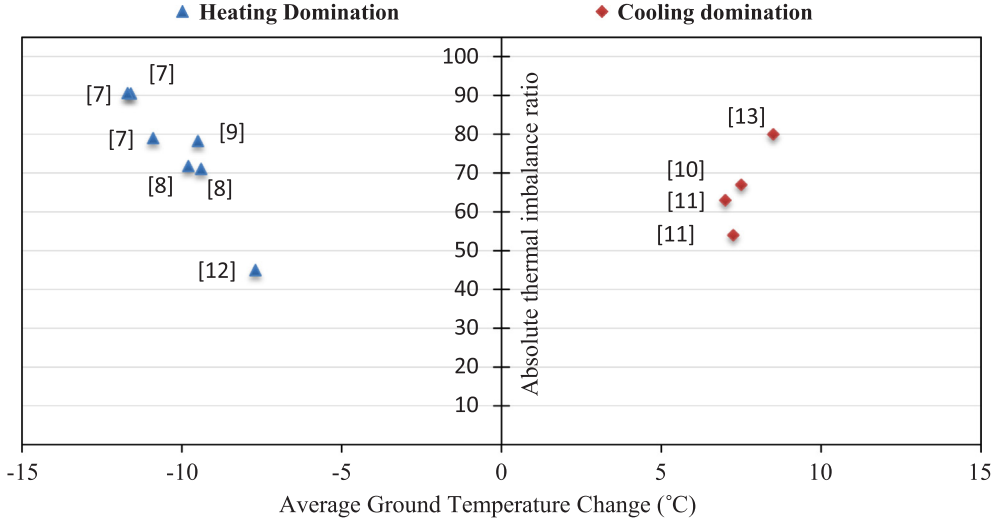

Fig. 2. Thermal imbalance influence of BTES [7–12]

a cooling operation is as high as 17.2 when ATES is used for heating and cooling, while the COP for cooling is 10.36 due to the additional storage of cold using the wasted heat from the heat pump. The thermal imbalance problem has not yet been studied for the ATES system.

Although the ATES and BTES systems show some differences in their operation, BTES and ATES are both ground heat storage systems with inter-season operation, which makes it possible to compare the two systems. Therefore, this literature survey focuses not only on ATES systems but also on BTES systems in order to point out the thermal imbalance effect on the system. Previous studies concerning the thermal imbalance problem in BTES conclude that the imbalance ratio has a considerable influence on the overall ground temperature. Because the heat is extracted and injected from the same field, the ground temperature decreases/increases steadily year by year. Studies ([7–12] have shown that the ground temperature can change in the range of ± 10 °C after 10 years of operation (Fig. 2). There is a certain trend between the amount of thermal imbalance and the average ground temperature change. It is also possible to see (Fig. 2) that there are small deviations between the cases with the same amount thermal imbalance such as [7,9]. Those kind differences are also related certain design parameters such as the number of boreholes, the spacing between borehole and thermal properties of both borehole and ground, which differs depending on the application. More detailed information can be found in those studies [7–12].The influence of thermal imbalance on the source temperature differs in ATES systems due to the separation of the heating and cooling source, which needs to be investigated.

The existing studies [6,20–22] that conduct simulation studies for the ATES system have been mostly implemented in TRNSYS. The authors in [6,20,22] use TRANSAT for an ATES model that is developed for TRNSYS. However, TRANSAT is not commercially or non-commercially available anymore. The authors in [21] develop a C code for the ATES model, which has no public access. The authors in [16] have already given detailed information on the need for a dynamic ATES model based on the finite element method (FEM) and develop an ATES model that is able to address the time dynamics imposed by a building load.

Co-simulation is a known approach for building energy management systems in buildings. Popular co-simulation approaches can be found in previous studies, such as Energy Plus with Java [23], Energy Plus with MATLAB and Energy Plus with computational fluid dynamics (CFD) [24,25]. However, a co-simulation approach toward CFD in connection with TRNSYS is a relatively new concept. The effectiveness of this method has been proven by Ferroukhi et al. [26]. TRSNYS has been frequently used to form complex energy flow diagrams within ATES systems in previous studies [6,20,22]. COMSOL has also been proven as an effective tool to solve a FEM-based numerical model of an ATES system [16]. Since, a new simulation platform is needed to enable the analysis of ATES within a system under the thermal imbalance concept, we first develop and present a new co-simulation method consisting of the tools namely COMSOL, MATLAB and TRNSYS that simulates ATES connected to a building load.

3. Methodology

3.1. Co-simulation platform

In this study, we combined TRNSYS, used for HVAC system modeling, and COMSOL, used for the ATES model. More detailed information on how the co-simulation works is given in Section 3.5. The system was simulated based on the coupling of three simulation softwares: TRNSYS 17, MATLAB and COMSOL. TRNSYS 17 was used to form the whole energy flow diagram, including the components of the building and heating/cooling systems (see Fig. 3), and COMSOL was used to model ATES. Information was exchanged between COMSOL and TRNSYS through MATLAB (acting as a master). Depending on the building load information, MATLAB activates one well group in charging mode and the rest of the wells in discharging mode.

3.2. Case study

The developed model was based on a case study of an office building in the Netherlands. The building has a total area of 3,520m^2. Due to the fact that ATES systems only started to be applied after the 1980 s [27], an energy flow diagram (Fig. 4) was applied and adapted for buildings of the same size built in 1980–1990, 1990–2000 and 2000–2010. U values (Table 1) were selected and applied based on the statistical average values applied to Dutch buildings in compliance with the build year [28]. This is intended to show the influence of the different building load profiles on the ATES ground source well temperatures.

There are two horizontally positioned wells integrated into the system and working in cyclic conditions. The operation is switched

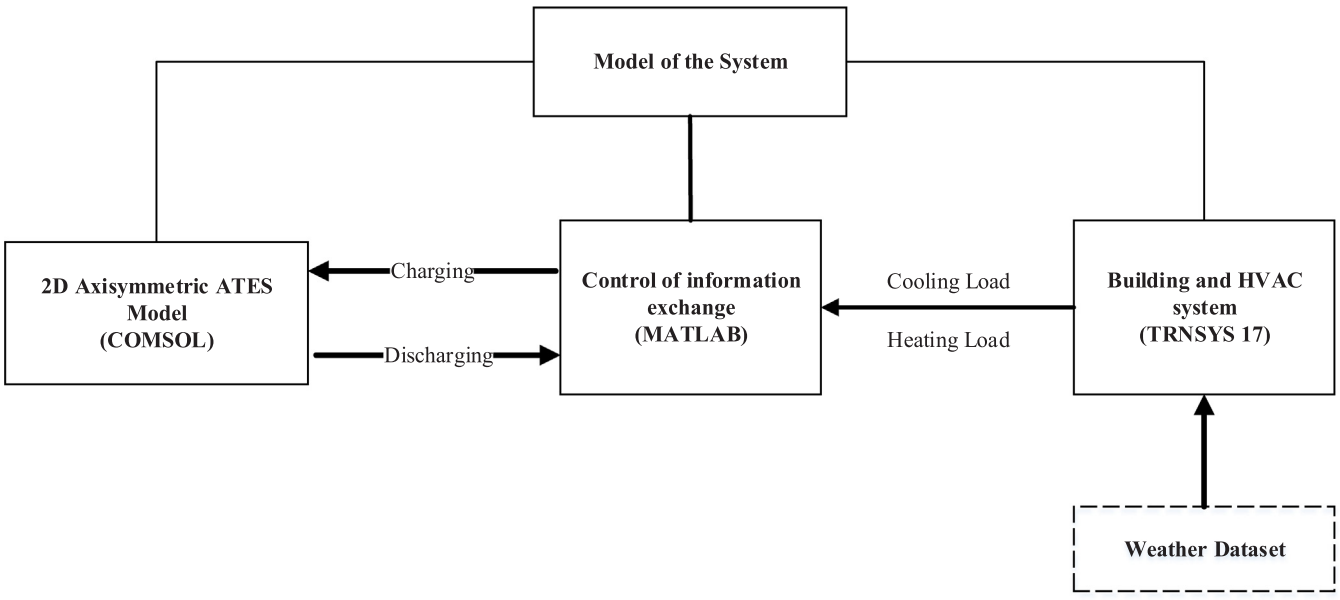

Fig. 3. Applied co-simulation method.

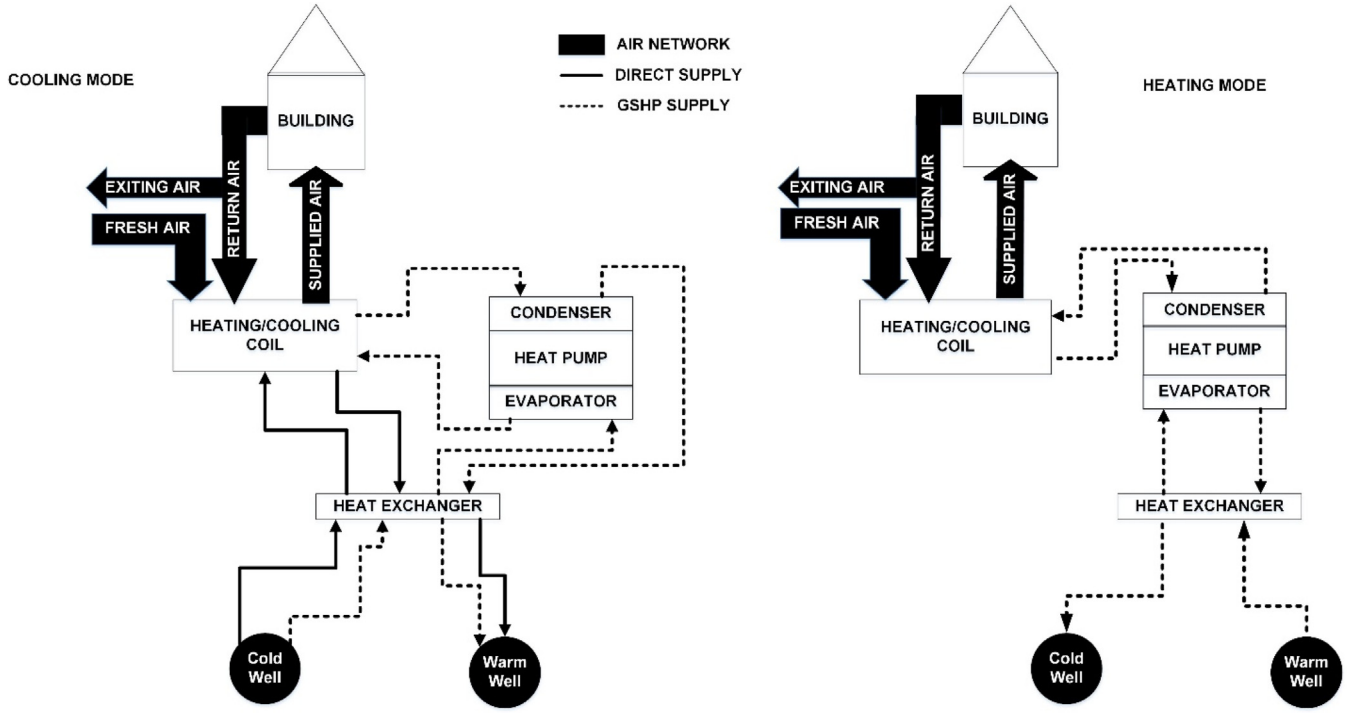

Fig. 4. Workflow of the aquifer and HVAC integrated system.

Table 1
U values for the cases.

Case/U values	Wall	Window	Floor	Roof
1980–1990 building	0.8	2.6	1.1	0.5
1990–2000 building	0.6	2.3	1.0	0.3
post-2000 building	0.6	2.1	0.7	0.3

depending on the season. In this study, the ATES system was designed to work in 16 °C heating and 8 °C cooling well operation temperatures at a ground temperature of 12 °C, presenting a typical application in the Netherlands [1,29]. Since ATES was hydraulically decoupled by a heat exchanger from the building side, the flow rate was adjustable in order to inject heat at the desired temperature into the wells. Depending on the inlet temperature to the wells, the proportional controller modulated the flow rate.

The system has three operational modes (Fig. 4): heating with heat pump (HP), direct cooling with ATES, and cooling with HP.

Heating with HP: The heat pump in connection with an air handling unit (AHU) and an ATES system is used to meet the entire heating/cooling demand of the building. During the heating season, the warm well provides heat for the evaporator of the heat pump, and chilled water is injected back into the cold well. Simultaneously, the building is heated up, and the cold well is being charged.

Direct cooling with ATES: In the cooling period, when the ambient air usually exceeds 13 °C, ATES directly extracts heat from incoming air through the cooling coil and injects the heat into the warm well.

Cooling with HP: If the cooling demand is not met, the outlet water from the cold well is pumped into the evaporator to further cool down the temperature supply to the cooling coil when the heat pump operates in chiller mode. The returned water from the cooling coil further extracts the heat at the condenser and finally re-injects all the heat into the warm well.

The office building operates during normal working hours from 7 a.m. to 6 p.m. on weekdays. ASHRAE Standard [30] was used to determine the occupancy rate for each hour, whereas no occupancy was considered during the weekend. The AHU was responsible for the distribution of heating and cooling. The heating temperature for the building was set at 21 °C with a ± 2 °C temperature dead band for the HP. In practical applications, the indoor cooling set point temperature for direct cooling supply is set to lower value than the set point for HP operation in cooling mode. By doing so, Direct cooling mode operates before HP to satisfy the cooling demand. In this study, the cooling control was set to 22 °C with ± 2 °C for the ATES and 24 °C ± 2 °C for the HP; therefore, the inside temperature was floating around 21.5 in the heating season and 24 °C in the cooling season. By setting the set point lower for the direct cooling supply, it was guaranteed that HP would operate when ATES was not sufficient, which was significant to assess the effect of the thermal quality of water on the performance of the system. The damper embedded in the AHU was controlled to limit the fresh air supply to a rate of 13.5 (L/s) per occupant, which is the needed amount for an office environment according to standards. In order to make a fair comparison between seasons, the starting simulation time was set to the first day of the cooling period; therefore, the warm well was primarily being charged in all simulations.

In this study, the return water temperature from the building side was designed in the range of 4–8 °C, while the cooling network was designed as 18–30 °C (Table 2), as it is practically applied [6];

Table 2
Physical parameters of ATES.

Physical conditions	Values	Unit
Hydraulic conductivity	$5x10^{-4}$	m/s
Thermal conductivity of aquifer	2.5	W/(m°C)
Initial ground temperature cold well	12	°C
Mean ambient temperature	10.4	°C
Effective porosity	35	%
Thickness of aquifer	10	m
Volumetric heat capacity of aquifer	2.45	MJ/m^3K
Operational conditions	Values	Unit
Injection/extraction flow rate of warm well (adjustable)	0–200	m3/h
Injection/extraction flow rate of cold well (adjustable)	0–200	m3/h
Injection temperature in heating season	8	°C
Injection temperature in cooling season	16	°C

therefore, the system could inject a temperature of 8 and 16 °C into the wells by adjusting the flow rate on the ATES side. The reason for the high return temperature in the chiller mode is due to the heat exchange on both the ATES and the condenser sides of the heat pump.

3.3. TRNSYS for building and HVAC modeling

The building was simulated using type 56, a multi-zone building model implementing actual building specifications. The AHU was modeled using type 600, which represents the central heating/cooling and air supply of a building with constant flow rate and power. The heat pump was modeled using TRNSYS type 927, which is applicable for groundwater source heat pumps. The HP model was calibrated using a manufacturer's datasheet with flow rate, heating/cooling power, and capacity. Components were controlled using differential controllers (type 4). Differential controllers were used to control the set-point temperature of the indoor air, the percentage of fresh air supply and the flow rates of the circulated water. A proportional controller (type 1669) was used to modulate the pump operation on the aquifer side.

Due to the different modes of operation in the system, there were many flow diverters and flow mixers in the hydraulic scheme. Control signals were assigned to the pumps and flow diverters (type 647) to activate the necessary pipelines. The colored[1] lines show the water pipeline network and the rest of the lines in Fig. 5.

3.4. COMSOL for aquifer modeling

The ATES model was numerically solved using the FEM. The model used in [31] was used for this paper as well. The flow of water in porous media was solved according to the Darcy law and coupled to heat transfer functions to determine the temperature distribution throughout the meshed domain.

The flow flux of water is written as a function of head gradient and coefficient of hydraulic conductivity:

$$\vec{q} = -\boldsymbol{K}\vec{\nabla}h \tag{1}$$

Transient drawdown on the injection/extraction is presented with the following equation:

$$\rho S_s \frac{\partial p}{\partial t} = Q_s - \vec{\nabla}(\rho q \tag{2}$$

Mass transfer in a porous medium is defined by the Darcy law. For homogenously distributed ground properties, hydraulic conductivity is distributed uniformly, or isotropically. The groundwater mass conservation equation is described by the following equation.

$$[\vec{\nabla}.(K\rho\vec{\nabla}h)]dV = Q_s \tag{3}$$

The full heat transfer equation including conduction and convection is derived from the Fourier and Darcy law, as shown in the following:

$$(pc)_s \frac{\partial T}{\partial t} = \vec{\nabla}((pc)_{aq}(\lambda_{aq})\vec{\nabla}T(r)) - (pc)_f\vec{\nabla}(q(r)T(r)) + Q_s \tag{4}$$

The following conditions (Table 3) were applied.

3.5. TRNSYS-MATLAB-COMSOL co-simulation

In this study, co-simulation with three softwares, MATLAB, COMSOL and TRNSYS, was conducted. Using the MATLAB component (type 155) of TRNSYS, it was possible to call external functions written in a MATLAB script. MATLAB has a toolbox that enables a connection with COMSOL. With this toolbox, MATLAB commands were able to run on a COMSOL server. Thus, MATLAB was responsible for the information exchange between the software, playing a mediating role. However, type 155 was not capable of identifying COMSOL scripts in MATLAB. Therefore, the connection between TRNSYS and COMSOL was decoupled, synchronized and solved separately. Information was exchanged through a common database provided in text files.

The co-simulation framework is shown in Fig. 6. The co-simulation was controlled by MATLAB and transferred input information from TRNSYS depending on the last updated status information in the file. By doing so, TRNSYS did not take a step before COMSOL found a solution for the domain and printed it to the file. The information was exchanged through text files. TRNSYS solves input variables based on the formed energy flow network and provides output variables for COMSOL through text files. COMSOL implemented the output from TRNSYS and sent the calculated output back to TRNSYS, thereby forming the whole cycle.

Warm and cold well models were described in COMSOL in connection with MATLAB. As shown in Fig. 7, COMSOL needed the information from TRNSYS, including inlet water temperature, inlet flow rate and the percentage of discharge pump, to calculate the heat transfer in the aquifer. Warm well and cold well signals were used to decide which well was in charging or discharging mode.

Thus, warm and cold well models simultaneously implemented the input variables and sent outputs, including the outlet water temperature and flow rate, back to TRNSYS through component type 155. The inlet temperature and flow rate to ATES were dependent on the cooling/heating load required for the building. COMSOL solved the models simultaneously based on the temperature and flow rate defined by the dynamic boundaries. In turn, warm well and cold well temperatures were provided as outputs, and TRNSYS returned the system with the temperature from either the cold well or the warm well, depending on the mode of operation.

The order of information exchange was important for the convergence and communication between COMSOL and TRNSYS. Adding a MATLAB component into such a complex system may cause false information exchange and synchronization problems between COMSOL and MATLAB. To avoid this problem, the order of information exchange between components was arranged in the order of heat transfer between components in TRNSYS. In this system, first the building load was calculated along with the required heat or cold transfer based on the control signal. The HVAC components' order was arranged depending on the circulation system. Lastly, MATLAB was responsible for the information exchange.

3.6. Performance indicators

The imbalance ratio of the building load differs from the ground side and depends on the components in the system. Therefore, in this study, the degree of imbalance was expressed using the imbalance ratio (IR), which is determined from the amount of energy extracted from the ground [5].

$$\boldsymbol{IR} = \frac{\boldsymbol{Q_{inj}} - \boldsymbol{Q_{ext}}}{\mathbf{max}(\boldsymbol{Q_{inj}}, \boldsymbol{Q_{ext}})} \times 100\% \tag{5}$$

By using this equation, the thermal imbalance was calculated based on the temperature difference between the outlet of the warm well and the inlet of the cold well.

The percentage of the well pump varies depending on the temperature difference between the warm and cold well and the amount of heat transfer with the building.

$$W_{pump,ww} = \frac{Q_b}{Cp_{water}(T_{ww} - 8)} \tag{6}$$

$$W_{pump,cw} = \frac{Q_b}{Cp_{water}(16 - T_{cw})} \tag{7}$$

The simulation starting time was set to the first cooling operation

[1] For interpretation of color in Fig. 5, the reader is referred to the web version of this article.

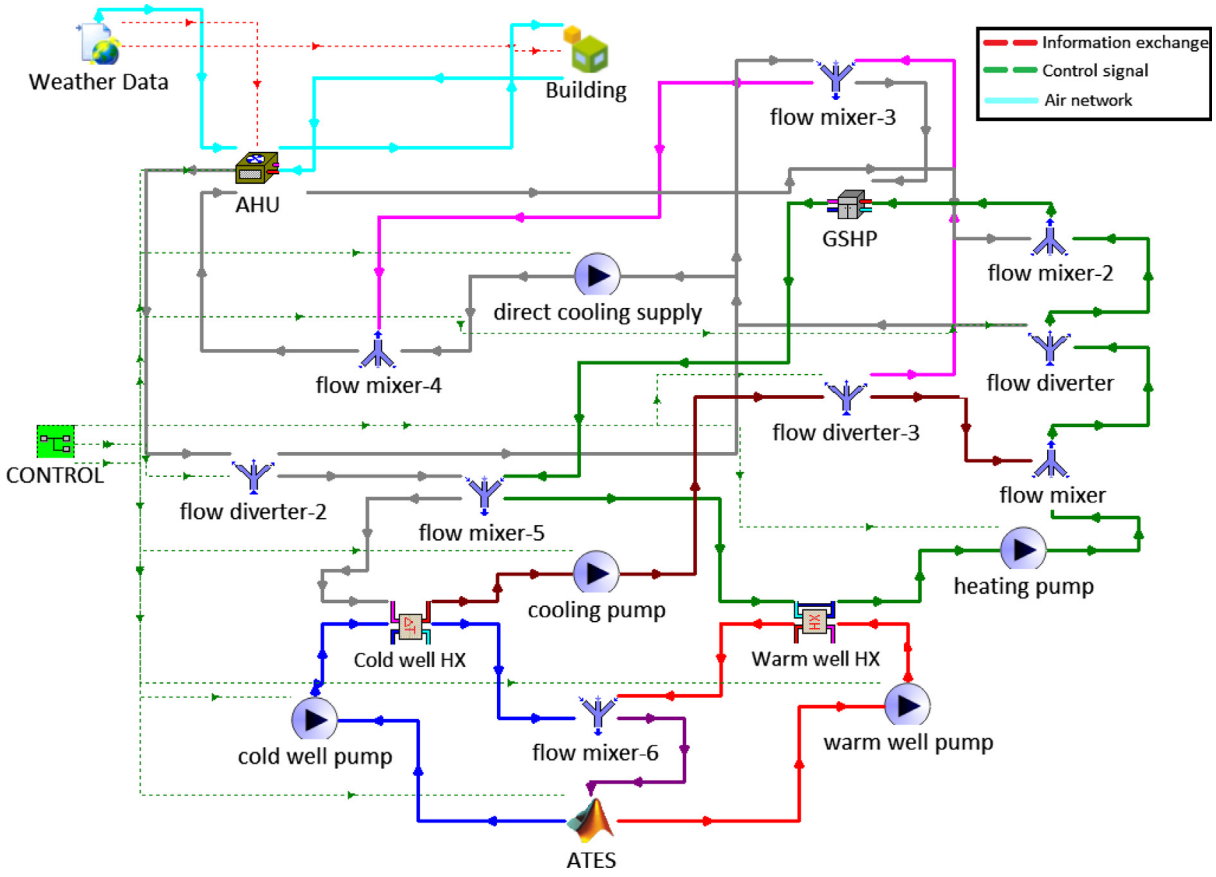

Fig. 5. Energy flow diagram in TRNSYS.

Table 3
Design results for the system.

Parameter	Unit	Value
Inlet temperature to AHU on direct cooling	°C	13–15
Inlet temperature to AHU in HP mode	°C	8–10
Inlet temperature to heating network	°C	35–40
Return temperature from cooling network on direct cooling	°C	18–20
Return temperature from cooling network in GSHP mode	°C	20–30
Return temperature from cooling network on heating	°C	4–8

time in order to make a fair comparison between the temperature changes of the warm and cold wells. Thus the system COP for heating and cooling, COP_{sys}, is calculated based on the ratio between the energy extracted from the fan coil and the total electricity consumption in one heating/cooling season. In addition, HP cooling, HP heating and direct cooling hours were calculated and changes were projected for a 10-year period.

$$W_{pump,ww} = \left(\left(\frac{Q_b}{Cp_{water}(T_{ww}-8)}\right)/V_{max}\right)W_{max} \quad (8)$$

$$W_{pump,cw} = \left(\left(\frac{Q_b}{Cp_{water}(16-T_{cw})}\right)/V_{max}\right)W_{max} \quad (9)$$

$$COP_{cooling} = \frac{Q_{cool}}{W_{fans} + W_{pump,cw} + W_{hp}} \quad (10)$$

$$COP_{heating} = \frac{Q_{heat}}{W_{fans} + W_{pump,ww} + W_{hp}} \quad (11)$$

$$COP_{sys} = \frac{Q_{cool} + Q_{heat}}{W_{fans} + W_{pump,cw} + W_{pump,ww} + W_{hp}} \quad (12)$$

4. Results

4.1. Thermal imbalance

Heat transfer rates to the ground were presented for each case, as shown in in Fig. 8. The case buildings, 1980–1990, 1990–2000 and post-2000 building presented the annual absolute heat transfer of 774, 558 and 442MWh to the ground, respectively, which were named as balanced case, case 1 and case 2, respectively. As can be observed, as the insulation within the building increases, the amount of heat exchange with the ground decreases due to the lower building demand. During the heating period, heat is directly exchanged with the evaporator. Since the heat pump is working with a fixed load, the amount of the extracted heat from the ground is in the rated heating capacity of the heat pump, which slightly varies depending on the COP. On the other hand, the heat injection rates vary greatly due to the direct heat exchange between the supply water and the indoor air temperature.

For the balanced case, the cooling capacity of ATES along with heat pump can reach a capacity of 250 W/m^2, which can be two to three

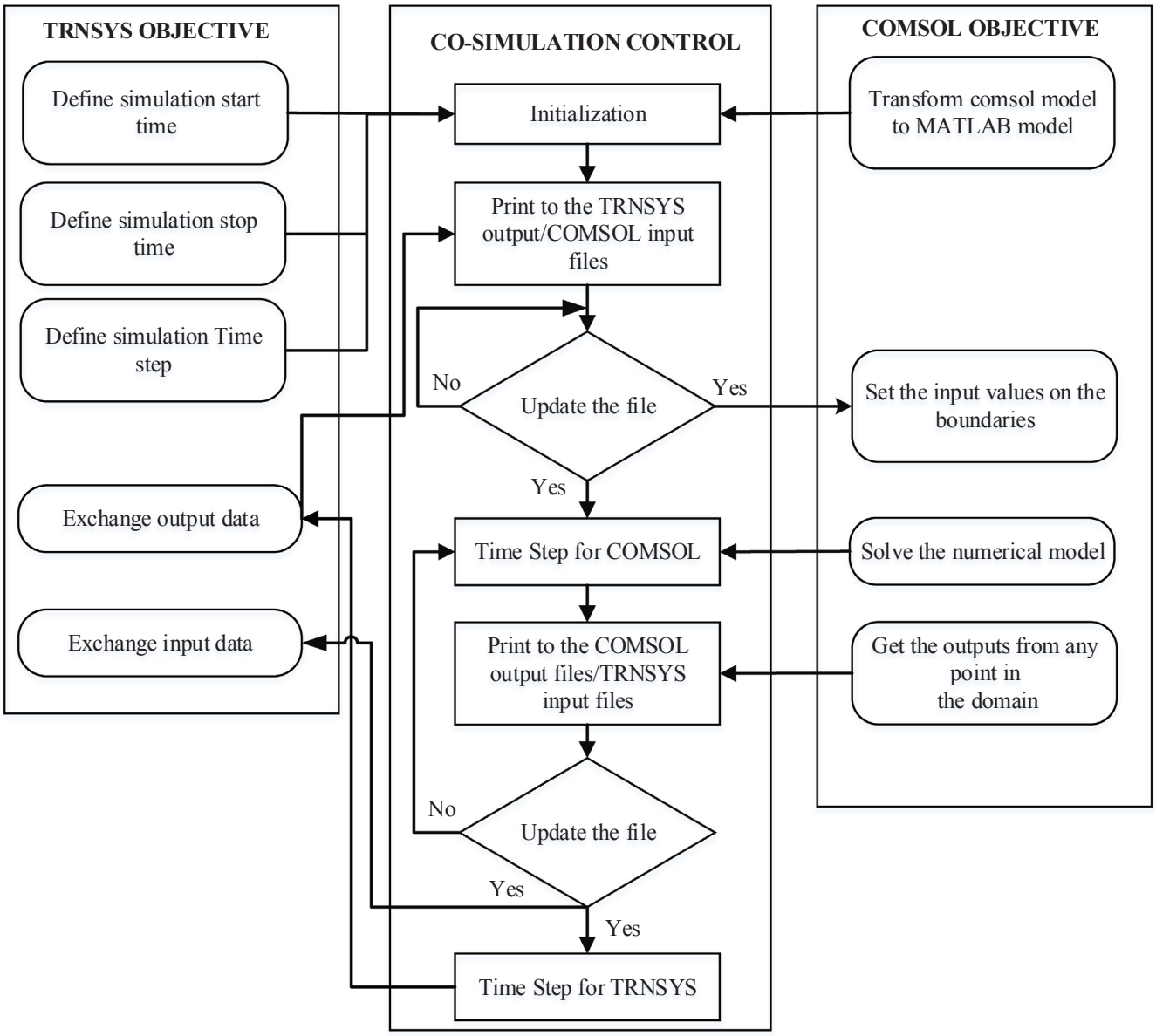

Fig. 6. Schematic diagram of the co-simulation framework.

times higher than the capacity of the heat pump [5]. The heat pump was sized based on the peak cooling/heating demand, which resulted in the rated capacities of 95, 70 and 60W/m^2 of HP, which in turn resulted in a relatively higher cooling capacity for the balanced case and case 1 in relation to the size of HP. Eventually, the thermal imbalances in the amount of heat transfer to the ground were determined to be 79%, 51% and -5.3% for case 2, case 1 and the balanced case, respectively.

4.2. Temperature

The dynamic yearly averaged and hourly groundwater temperature trends are presented in Figs. 9 and 10. The cases (Fig. 8) presented 180, 200 and 230 days of the cooling season for the balanced case, case 1 and case 2, respectively. While the average extraction temperature is directly influenced by the thermal imbalance ratio, the yearly trend is influenced by the accumulation of heat/cold. The increases in temperature in case 1 and case 2 for the cold well were quite small, since there was a very small amount of surplus cold from year to year. Specifically, there was a higher gradient in the first four years of operation due to the higher increase in the temperature for all cases [32]. The average extracted cold well temperatures were determined to be 8.4, 9.9 and 10.9 °C, respectively, at the end of the 10th year.

Fig. 11 presents the temperature distribution in the 2D axisymmetric domain at the end of the 10th charging period. It can be seen that the domain size was sufficient to simulate total heat/cold injection. The thermal imbalance was visible for each case. The thermal front for warm well reaches as far as 300 m, 175 m and 90 m for case 2, case 1 and the balanced case at the end of the 10th year operation, respectively. The thermal front for the cold well was as low as 50 m.

It can be clearly observed that as the thermal imbalance ratio increased for the cooling-dominated loads, the cold-well temperature was significantly influenced (Figs. 9 and 10). The balanced thermal load maintained the highest overall thermal potential for both wells, where the system achieved a temperature difference of 7.6 °C. Case 1 and case 2 saw a temperature difference of 6.1 and 5.1 °C, respectively, at the end of the 10 years of operation.

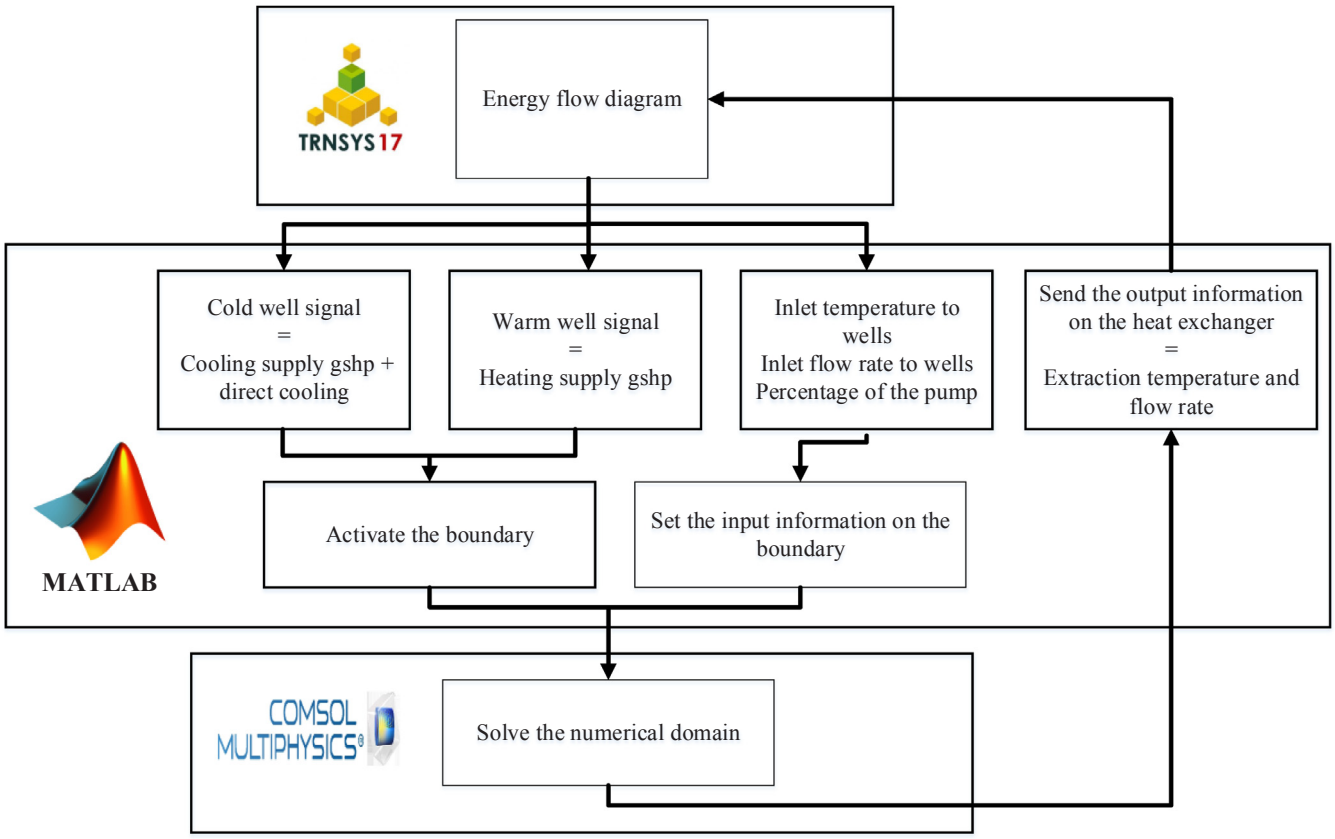

Fig. 7. Information exchange between COMSOL and TRNSYS.

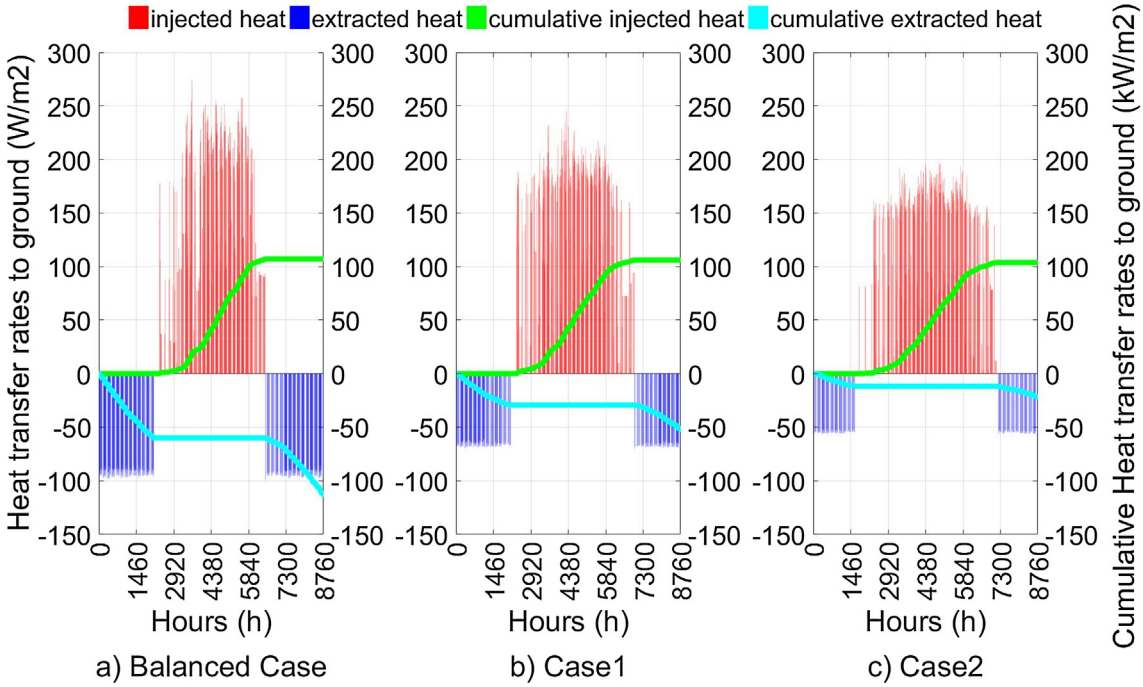

Fig. 8. Hourly heat transfer in three cases.

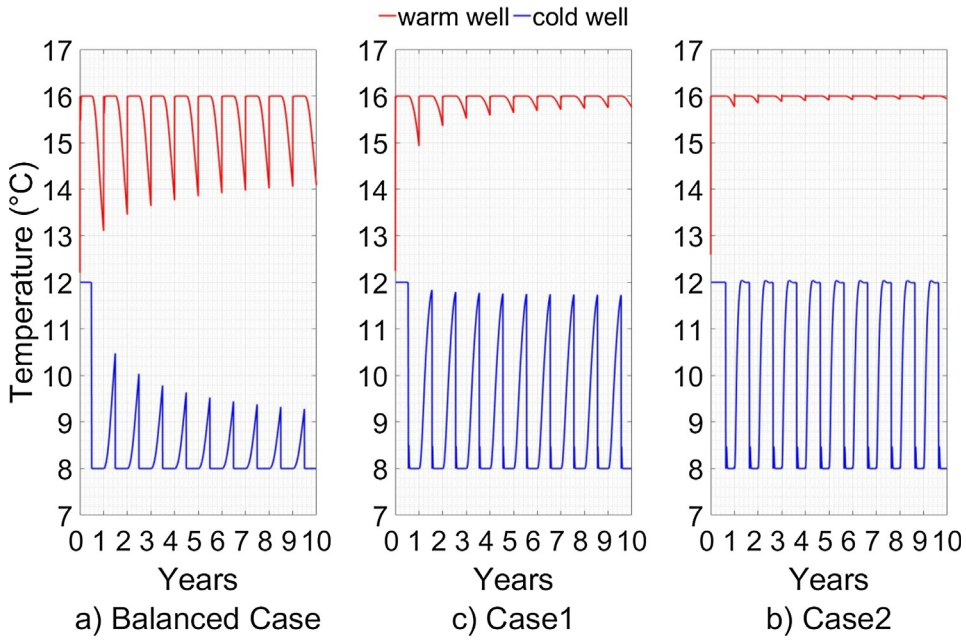

Fig. 9. Hourly temperature changes in wells.

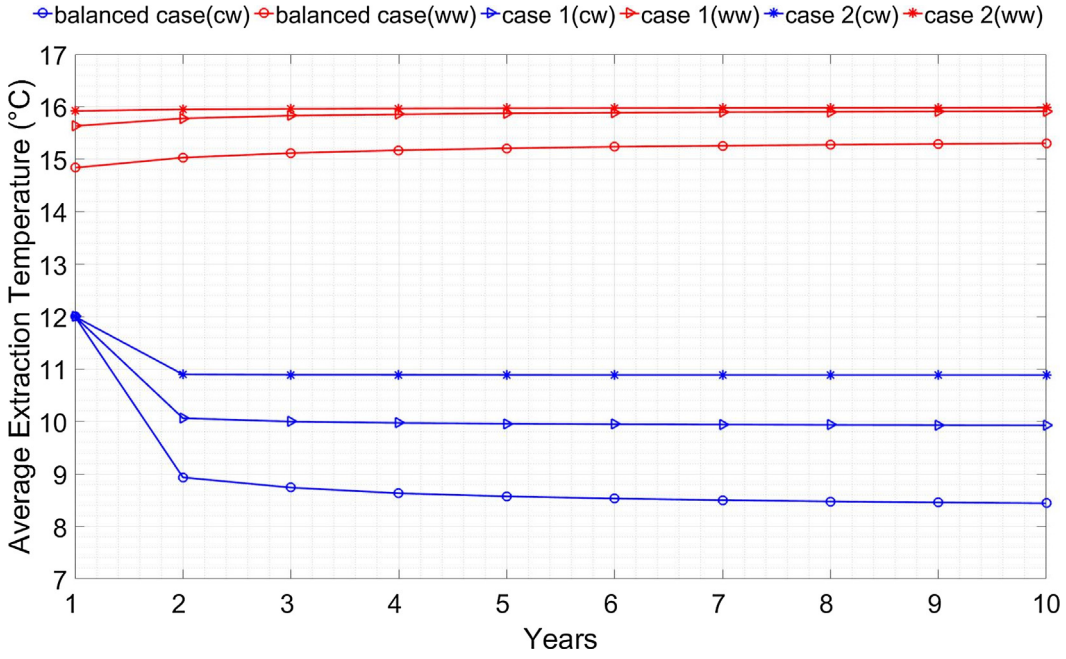

Fig. 10. Yearly averaged extraction temperature; cw stands for cold well and ww stands for warm well.

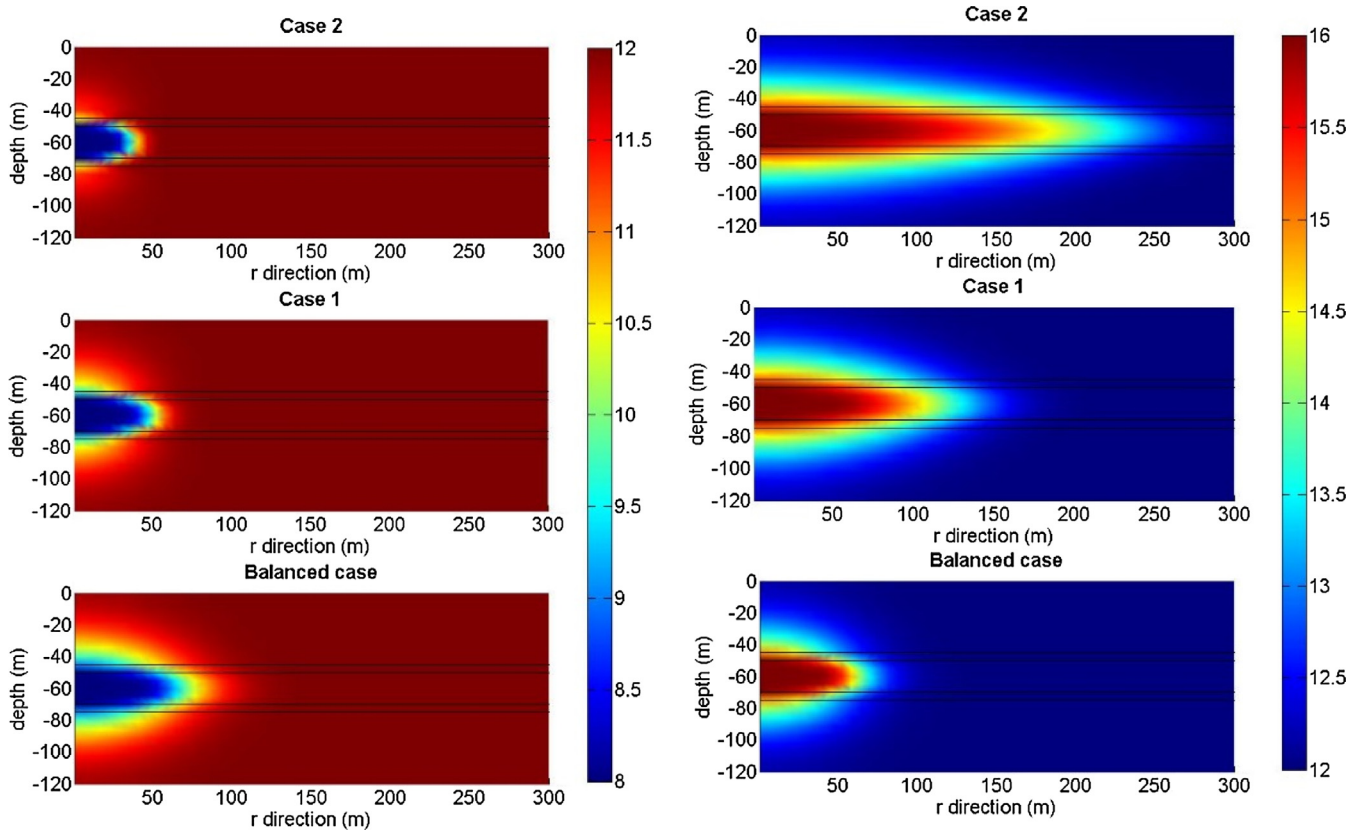

Fig. 11. Temperature distribution for cold well (left) and warm well (right).

Table 4
Power consumption of the well pump.

Case/Average power consumption (kWh)	$W_{pump,ww}$	$W_{pump,cw}$
balanced case	4.7	6.9
case 1	4.4	9.5
case 2	4.4	12.2

4.3. System performance

The system performance was analyzed based on the supply temperature from ATES. In order to eliminate the influence of the system design parameters, the supply temperature of ATES for case 1 and the balanced case were also applied to the building in case 2 in order to make a fair comparison. As shown in Eqs. (6) and (7), the power

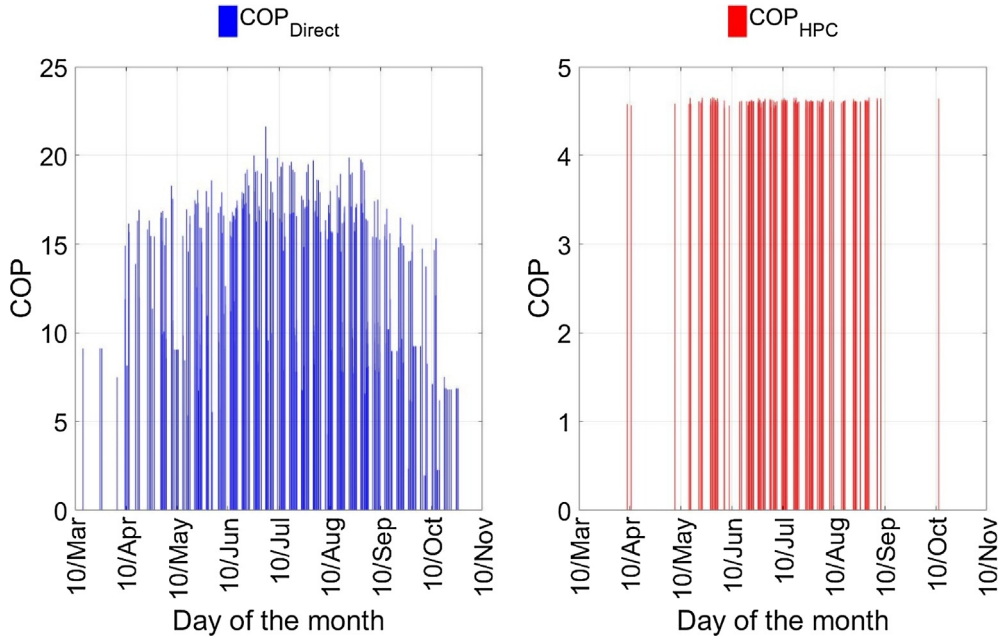

Fig. 12. Hourly COP values of direct cooling and heat pump for case 2.

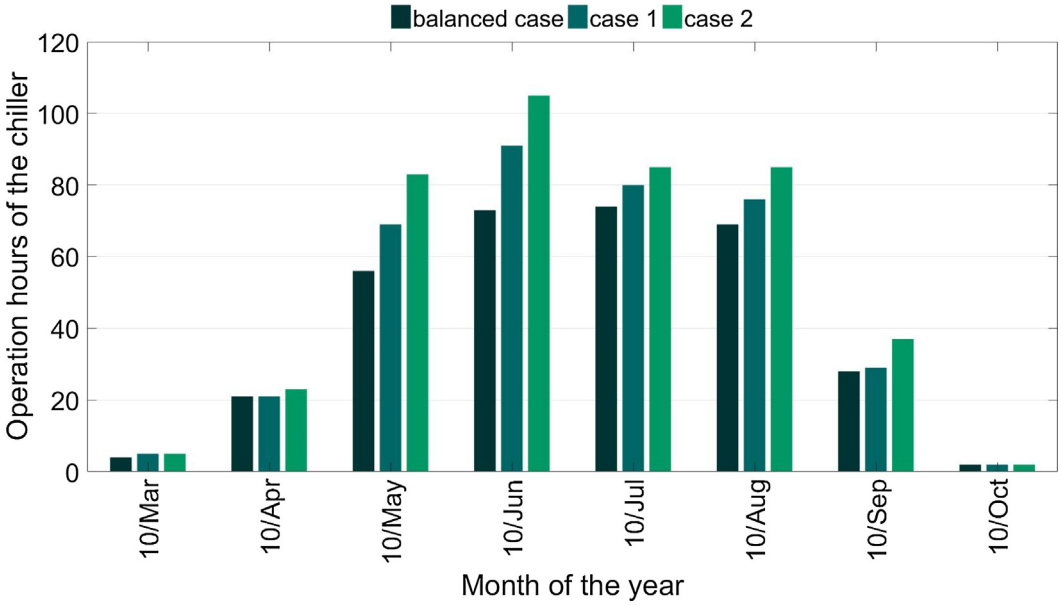

Fig. 13. Comparison of the chiller operation.

consumption of the well pump varies. Since the well pump is modulated to be able to inject 16 °C and 8 °C water for the wells, the energy consumption of the pump varies depending on the temperature levels of the wells and the heat transfer rate. It is possible to see (Table 4) that $W_{pump,ww}$ varied very slightly, since the warm well temperature did not change significantly. However, there is an obvious difference for $W_{pump,cw}$ due to the change in cold well temperature. Since the supply temperature from the cold well is the highest (lowest temperature difference), $W_{pump,cw}$ is the highest and decreases as the cold well temperature decreases.

Since the chiller operation hours decreased, there was a noticeable improvement in $COP_{cooling}$ as well. Fig. 12 presents the COP values of direct supply of cooling (COP_{direct}) and of the heat pump in chiller mode (COP_{HPC}). Since the direct supply of cooling was in the cost-of-pump operation, direct supply achieved a higher COP than the heat pump in chiller mode. It is also seen in Fig. 12 that the heat pump was working more frequently during the middle of the cooling period as the cooling demand rates of the building increased. COP_{HPC} varies slightly due to the small variations in cooling capacity of the heat pump, while COP_{direct} varies widely depending on the supply temperature and the indoor temperature of the building.

Fig. 13 presents the change in the number of heat pump operations in chiller mode. In relation to the temperature levels (Fig. 8), the system COPs for cooling ($COP_{cooling}$) and heating ($COP_{heating}$) were influenced. $COP_{cooling}$ was mainly influenced by the reduction of the chiller operation (Figs. 13 and 14). As expected, there is a noticeable difference between case 2 and the balanced case, due to the temperature difference in the cold supply temperature, where the $COP_{cooling}$ for the balanced case was 13.2 and 9.8 for case 2. On the other hand, $COP_{heating}$ was negligibly influenced, due to the small difference between the

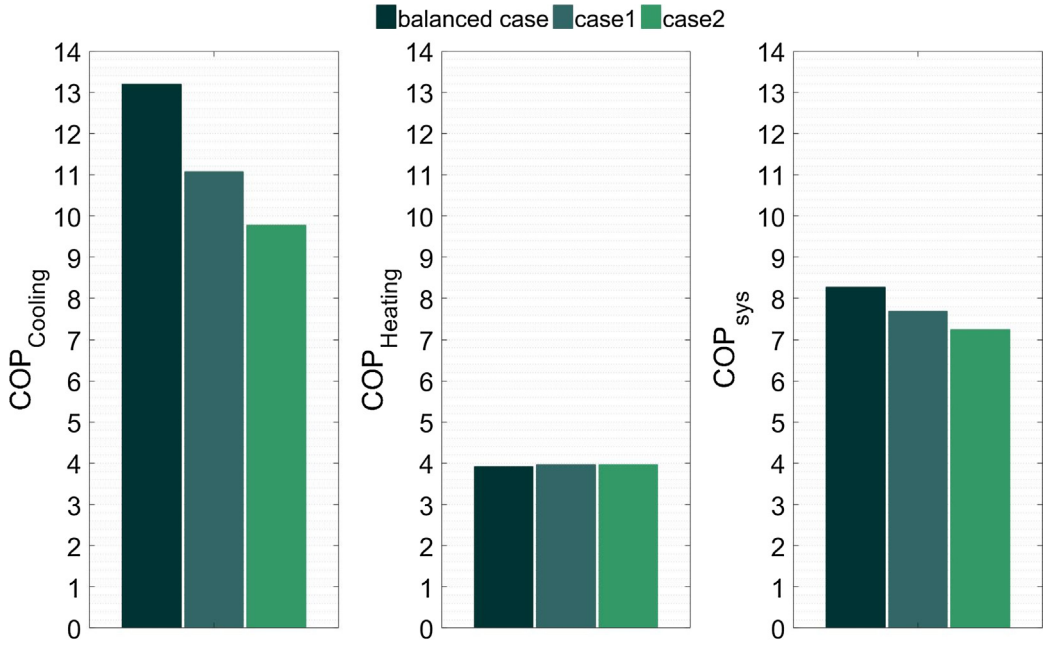

Fig. 14. Performance of the system.

warm-well temperature and the power consumption of the pump. Eventually, COP_{sys} was 8.3 for the balanced case, whereas it was 7.3 for case 2 at the end of the 10th year of operation.

5. Discussion

Thermal imbalances in the amount of heat transfer to the ground remain a subject that needs to be investigated for ground-sourced applications including BTES and ATES systems. Previous studies [8–12,22] mainly focus on BTES systems due to the broad application of the system. Since the heat is transferred to the same field in a BTES system, there is a direct interaction between cold and heat sources, and the source temperature from the ground is severely influenced, with the ground temperature changing in the range of ± 10 °C depending on the thermal imbalance ratio. In BTES systems, the accumulation of heat/cold results in steady decrease/increase in the temperature year by year. For ATES, however, it was observed that yearly temperature change is limited to the accumulation of heat and cold sources, which is also known as the change in heat recovery for each individual well. It was observed that there is a direct influence on the availability of heat and cold stored in the wells. For instance, a thermal imbalance ratio of 79% resulted in an average extraction temperature of 10.9 °C from the cold well. Considering the 16 °C of the injection temperature, the system operates under a 5.1 °C, 6.1 °C and 7.6 °C temperature difference for case 2, case 1 and the balanced case in the cold supply, respectively, while the expected temperature difference of the heat exchanger is at least 8 °C [2] in the Netherlands. This may result in a decrease in the direct cooling supply hours and even in a cooling problem during peak demand if the heat pump is sized based on the capacity of ATES in cooling supply. Similarly, Kranz et al. [16] determine a lower extraction temperature for a warm well and a higher extraction for a cold well than the designed temperature due to underestimated building demand.

As mentioned in previous studies [6,16,21], cold wells are an important natural source for cooling due to the suitable ground temperature, which also makes the system very sensitive to changes in the cold-well temperature. The decrease in the supply temperature from 10.9 °C to 8.4 °C increases the $COP_{cooling}$ from 9.6 to 12.3 due to the increase in the direct cooling share.

A co-simulation platform was developed in this study. The co-simulation method can be used for further investigation for other applications. The main limitation of this method in comparison to the one in previous studies [6,20,21] is the calculation period. Since COMSOL applies the FEM, this method can be more time-consuming in comparison with the finite difference model (TRANSAT) in TRNSYS and eventually requires more time and sources to be implemented. Besides, there are additional time losses due to the information exchange between the software. The advantage of this method is the reliability and the adaptability of both ATES and the TRNSYS model to the various ground and building conditions, which is also mentioned in [31]. In this paper, the thermal interaction between the well groups was neglected due to the fact that the current installations were installed with enough spacing. The thermal interaction may occur in the very long term and in a very high domination of a group of wells in the region [1]. The selected temperature settings for ATES are usually applied in the range of 16–18 °C for a warm well and 6–8 °C for a cold well in the Netherlands. The design parameters for operating conditions, such as the injection temperatures for well groups and indoor temperature settings, may vary depending on where the system is applied. Various ground conditions and operational parameters can be further investigated; however, that is out of the scope of this paper.

6. Conclusion

A co-simulation method using TRNSYS-MATLAB-COMSOL for integrating ATES modeling into building HVAC system modeling has been presented. The co-simulation method was applied to three cases. The thermal imbalance effect on temperature changes of ATES and the performance of the system was investigated. The following conclusions can be drawn from this study:

(1) The co-simulation method is capable of integrating ATES into a building-dynamic simulation, allowing the user to analyze system dynamics.
(2) Thermal imbalances have a direct influence on the temperature levels of the wells, which also affects the thermal potential of the cold and warm wells. Although the warm well is hardly influenced by cooling-dominated loads, the cold well temperature is significantly influenced by a 79% thermal imbalance ratio, where the average supply temperature from the cold well deviates by 2.5 °C from the balanced case.
(3) The cooling performance is highly sensitive to the cold supply temperature. A decrease of the cold well temperature by 2.5 °C decreases the $COP_{cooling}$ from 13.2 to 9.8 due to a decrease in the direct cooling supply share. Eventually, the COP_{sys} is 13.7% higher in the balanced case than in the case with a 79% thermal imbalance ratio and 6% higher than the case with 51%.

Overall, these results indicate that the thermal potential of ATES is influenced by thermal imbalance. While the current practices are designed with at least 8 °C between the cold and warm well, the temperature difference is as low as 5.1 °C for a building with a 79% thermal imbalance ratio in cooling supply, which leads to problems for the optimal design of the system and a decrease in overall performance of 13.7%. Therefore, the ATES integrated systems should be properly sized in accordance with building load and possible extraction temperature from the wells in order to maintain a reliable and energy-efficient system design.

References

[1] M. Bloemendal, T. Olsthoorn, F. Boons, How to achieve optimal and sustainable use of the subsurface for aquifer thermal energy storage, Energy Policy 66 (Mar.) (2014) 104–114.
[2] B. Nordell, A. Snijders, L. Stiles, 5 - The use of aquifers as thermal energy storage (TES) systems, Woodhead Publishing, 2015, pp. 87–115.
[3] X.Q. Zhai, M. Qu, X. Yu, Y. Yang, R.Z. Wang, A review for the applications and integrated approaches of ground-coupled heat pump systems, Renew. Sustain. Energy Rev. 15 (6) (2011) 3133–3140.
[4] G. Drenkelfort, S. Kieseler, A. Pasemann, F. Behrendt, Aquifer thermal energy storages as a cooling option for German data centers, Energy Effic. 8 (2) (2014) 385–402.
[5] D. Vanhoudt, J. Desmedt, J. Van Bael, N. Robeyn, H. Hoes, An aquifer thermal storage system in a Belgian hospital: Long-term experimental evaluation of energy and cost savings, Energy Build. 43 (12) (2011) 3657–3665.
[6] S. Kranz, S. Frick, Efficient cooling energy supply with aquifer thermal energy storages, Appl. Energy 109 (Sep.) (2013) 321–327.
[7] T. You, B. Wang, W. Wu, W. Shi, X. Li, Performance analysis of hybrid ground-coupled heat pump system with multi-functions, Energy Convers. Manag. 92 (Mar.) (2015) 47–59.
[8] W. Wu, B. Wang, T. You, W. Shi, X. Li, A potential solution for thermal imbalance of ground source heat pump systems in cold regions: ground source absorption heat pump, Renew. Energy 59 (Nov.) (2013) 39–48.
[9] T. You, B. Wang, W. Wu, W. Shi, X. Li, A new solution for underground thermal imbalance of ground-coupled heat pump systems in cold regions: heat compensation unit with thermosyphon, Appl. Therm. Eng. 64 (1) (2014) 283–292.
[10] R. Fan, Y. Gao, L. Hua, X. Deng, J. Shi, Thermal performance and operation strategy optimization for a practical hybrid ground-source heat-pump system, Energy Build. 78 (Aug.) (2014) 238–247.
[11] M. Yi, Y. Hongxing, F. Zhaohong, Study on hybrid ground-coupled heat pump systems, Energy Build. 40 (11) (2008) 2028–2036.
[12] Z. Liu, W. Xu, X. Zhai, C. Qian, X. Chen, Feasibility and performance study of the hybrid ground-source heat pump system for one office building in Chinese heating dominated areas, Renew. Energy 101 (Feb.) (2017) 1131–1140.
[13] Y. Man, H. Yang, J. Wang, Study on hybrid ground-coupled heat pump system for air-conditioning in hot-weather areas like Hong Kong, Appl. Energy 87 (9) (2010) 2826–2833.
[14] V. Somogyi, V. Sebestyén, E. Domokos, A. Zseni, Z. Papp, Thermal impact assessment with hydrodynamics and transport modeling, Energy Convers. Manag. 104 (Nov.) (2015) 127–134.
[15] J.-S. Jeon, S.-R. Lee, L. Pasquinelli, I.L. Fabricius, Sensitivity analysis of recovery efficiency in high-temperature aquifer thermal energy storage with single well,

Energy 90 (Oct.) (2015) 1349–1359.
[16] X. Xiao, Z. Jiang, D. Owen, C. Schrank, Numerical simulation of a high-temperature aquifer thermal energy storage system coupled with heating and cooling of a thermal plant in a cold region, China, Energy 112 (Oct.) (2016) 443–456.
[17] A. Yapparova, S. Matthäi, T. Driesner, Realistic simulation of an aquifer thermal energy storage: Effects of injection temperature, well placement and groundwater flow, Energy 76 (Nov.) (2014) 1011–1018.
[18] H.O. Paksoy, Z. Gürbüz, B. Turgut, D. Dikici, H. Evliya, Aquifer thermal storage (ATES) for air-conditioning of a supermarket in Turkey, Renew. Energy 29 (12) (2004) 1991–1996.
[19] B. Turgut, H.Y. Dasgan, K. Abak, H. Paksoy, H. Evliya, S. Bozdag, aquifer thermal energy storage application in greenhouse climatization, Acta Hortic. 807 (Jan.) (2009) 143–148.
[20] G. Drenkelfort, S. Kieseler, A. Pasemann, F. Behrendt, Aquifer thermal energy storages as a cooling option for German data centers, Energy Effic. 8 (2) (2015) 385–402.
[21] H. Ghaebi, M.N. Bahadori, M.H. Saidi, Performance analysis and parametric study of thermal energy storage in an aquifer coupled with a heat pump and solar collectors, for a residential complex in Tehran, Iran, Appl. Therm. Eng. 62 (1) (2014) 156–170.
[22] R.M. Zeghici, A. Damian, R. Frunzulică, F. Iordache, Energy performance assessment of a complex district heating system which uses gas-driven combined heat and power, heat pumps and high temperature aquifer thermal energy storage, Energy Build. 84 (Dec.) (2014) 142–151.
[23] T. Hong, H. Sun, Y. Chen, S.C. Taylor-Lange, D. Yan, An occupant behavior modeling tool for co-simulation, Energy Build. 117 (Apr.) (2016) 272–281.
[24] Z.J. Zhai, Q.Y. Chen, Performance of coupled building energy and CFD simulations, Energy Build. 37 (4) (2005) 333–344.
[25] Z. Zhai, Q. Chen, P. Haves, J.H. Klems, On approaches to couple energy simulation and computational fluid dynamics programs, Build. Environ. 37 (8–9) (2002) 857–864.
[26] M.Y. Ferroukhi, R. Djedjig, K. Limam, R. Belarbi, Hygrothermal behavior modeling of the hygroscopic envelopes of buildings: a dynamic co-simulation approach, Build. Simul. 9 (5) (2016) 501–512.
[27] A.L. Snijders, K. de Wit, Solar heating of a large office building using seasonal aquifer thermal energy storage, First E.C. Conference on Solar Heating, Springer, Dordrecht, 1984, pp. 958–962.
[28] "WP2_D2.1a_20140523_P18_Survey-on-the-energy-needs-and-architectural-features.pdf".
[29] J.S. Dickinson, N. Buik, M.C. Matthews, A. Snijders, Aquifer thermal energy storage : theoretical and operational analysis, Geotechnique 59 (3) (2009) 249–260.
[30] "ASHRAEASHRAE 90.1 Appendix G. Building Performance Rating MethodASHRAE (2004)".
[31] B. Bozkaya, R. Li, T. Labeodan, R. Kramer, W. Zeiler, Development and evaluation of a building integrated aquifer thermal storage model, Appl. Therm. Eng. 126 (Nov.) (2017) 620–629.
[32] M. Bakr, N. van Oostrom, W. Sommer, Efficiency of and interference among multiple aquifer thermal energy storage systems; a Dutch case study, Renew. Energy 60 (Dec.) (2013) 53–62.